ELSEVIER

Polymer 43 (2002) 7515–7520

polymer

www.elsevier.com/locate/polymer

Investigation of computer-aided engineering of silicone rubber vulcanizing (II)—finite element simulation of unsteady vulcanization field

Yuxi Jia*, Sheng Sun, Shuxia Xue, Lili Liu, Guoqun Zhao

School of Material Science and Engineering, Shandong University, Jinan 250061, People's Republic of China

Received 6 April 2002; received in revised form 26 September 2002; accepted 28 September 2002

Abstract

On the basis of construction of the mathematical model of vulcanization ratio and numerical calculation of crosslinking structure parameters and derivation of the control equation of temperature field, two-dimensional space is divided in the manner of triangular element, then the interpolating function is calculated. Thereafter, the calculation of the element variation and collectivity synthesis is done, and the procedures of the numerical simulation of vulcanization process are described in detail. Finally, the computer-aided engineering software of silicone rubber vulcanizing is designed. The rationality of the simulation theory is verified by hardness test and analytical test. © 2002 Elsevier Science Ltd. All rights reserved.

Keywords: Silicone rubber; Vulcanization process; Numerical simulation

1. Introduction

When liquid silicone rubber is used as mould material and rapid prototype such as LOM prototype is used as master model of vulcanization, the rapid tooling technology can greatly reduce production cost and shorten production period. So the technology becomes one of the investigation hotspots in the field of advanced manufacturing technology [1–6].

Therefore, it is important to investigate the numerical simulation theory and design the computer-aided engineering software of silicone rubber vulcanizing process. On the basis, the properties of silicone rubber mould can be forecasted and the crosslinking structure can be controlled based on forward simulation method, or the reaction parameters can be optimized and the original polymeric material can be designed based on backward simulation method.

2. Dividing two-dimensional space

For the area D with boundary Γ, as shown in Fig. 1, it is divided in the manner of triangular element, the number of elements is expressed as E. Every element has its sequence number ①, ②,…. The inner elements are numbered in advance, the outer elements with the third kind of thermal boundary condition are numbered sequentially, the outer elements with the fourth kind of thermal boundary condition are numbered finally.

The number of nodes is expressed as n, every node also has its sequence number 1,2,…. Each element connects with its adjacent elements through its three nodes. For every element, its three nodes are numbered by i, j and m in the counterclockwise direction. For simplicity, only one side, which is numbered by jm, locates on the boundary in every outer element, and the node i is opposite to the boundary.

3. Calculating interpolating function

An arbitrary element in area D is shown in Fig. 2. Because the coordinate figures of the three nodes are known (ascertained by the above discretization of two-dimensional space), the lengths S_i, S_j, S_m of the three sides jm, mi, ij and the area Δ of the element can be calculated. In finite element simulation, the temperature T of an arbitrary point (x, y) is dispersed to the three nodes. Namely, the temperature field of the element is expressed by the three nodal temperatures

* Corresponding author.
E-mail address: jia_yuxi@sdu.edu.cn (Y. Jia).

0032-3861/02/$ - see front matter © 2002 Elsevier Science Ltd. All rights reserved.
PII: S0032-3861(02)00705-X

Nomenclature

$f_{V,c}$	vulcanization ratio corresponding to gel point
$f_{V,i}$	ideal vulcanization ratio
$[K]$	stiffness matrix of temperature of collectivity
$[K]^e$	stiffness matrix of temperature of element
$[N]$	alternating temperature matrix of collectivity
$[N]^e$	alternating temperature matrix of element
N_l	shape function, corresponding to No. l node
$\{P\}$	column vector of collectivity, determined by reaction heat
$\{P_l\}^e$	column vector of No. l node in element, determined by reaction heat
p	coefficient of vulcanization intensity, correlated with temperature and element, K^{-1}
q	constant coefficient of vulcanization intensity, correlated with element
q_2	heat-flow density through boundary between silicone rubber and LOM prototype (W m^{-2})
S_l	length of element boundary, corresponding to No. l node (m)
T_l	temperature of No. l node (K)
$\{T\}_t$	column vector of temperature at time t (unknown)
$\{T\}_{t-\Delta t}$	column vector of temperature at time $t-\Delta t$ (known)
t_{90}	optimum vulcanization time (s)
W_l	weighting function of No. l node
x_l	abscissa of No. l node (m)
y_l	ordinate of No. l node (m)
Δ	area of triangular element (m^2)

T_i, T_j and T_m, as shown below

$$T = f(T_i, T_j, T_m) \tag{1}$$

The treatment is called after discretization of temperature field, Eq. (1) is called after interpolating function.

In order to obtain the specific form of the interpolating function, Eq. (1) should be calculated based on the principle of discrete mathematics.

Linear interpolating function is the simplest one in finite

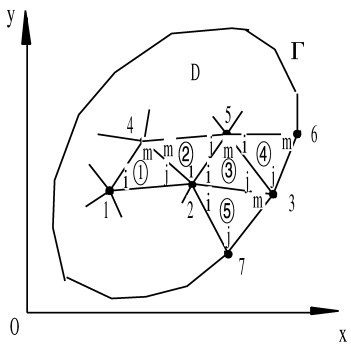

Fig. 1. Discretization of two-dimensional space.

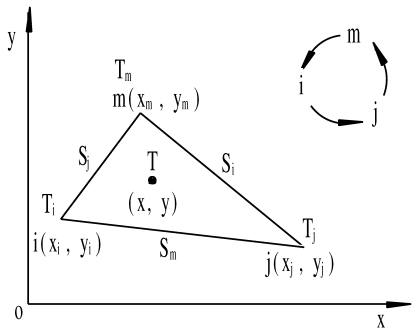

Fig. 2. Discretization of temperature field.

element method. If the element is enough small, its error becomes small enough to satisfy the accuracy requirement [7–9]. Therefore, the linear interpolating method is adopted.

The temperature T of an arbitrary point (x, y) is defined as the linear function of coordinate figures x, y

$$T = a_1 + a_2 x + a_3 y \tag{2}$$

where a_1, a_2, a_3 are undetermined coefficients. The coordinate figures and temperatures of the three nodes are fit into Eq. (2), then it is converted into matrix function, a_1, a_2, a_3 can be achieved by matrix inversion method

$$a_1 = \frac{1}{2\Delta}[(x_j y_m - x_m y_j)T_i + (x_m y_i - x_i y_m)T_j + (x_i y_j - x_j y_i)T_m] \tag{3}$$

$$a_2 = \frac{1}{2\Delta}[(y_j - y_m)T_i + (y_m - y_i)T_j + (y_i - y_j)T_m] \tag{4}$$

$$a_3 = \frac{1}{2\Delta}[(x_m - x_j)T_i + (x_i - x_m)T_j + (x_j - x_i)T_m] \tag{5}$$

Eqs. (3)–(5) are fit into Eq. (2), then it is converted into matrix equation

$$T = \begin{bmatrix} N_i & N_j & N_m \end{bmatrix} \begin{Bmatrix} T_i & T_j & T_m \end{Bmatrix}^{\mathrm{T}} = [N]^e \{T\}^e \tag{6}$$

where

$$N_i = \frac{1}{2\Delta}[(x_j y_m - x_m y_j) + (y_j - y_m)x + (x_m - x_j)y] \tag{7}$$

$$N_j = \frac{1}{2\Delta}[(x_m y_i - x_i y_m) + (y_m - y_i)x + (x_i - x_m)y] \tag{8}$$

$$N_m = \frac{1}{2\Delta}[(x_i y_j - x_j y_i) + (y_i - y_j)x + (x_j - x_i)y] \tag{9}$$

N_i, N_j, N_m are called after shape functions.

4. Derivation of element variation equation

When the number of elements is enough large and the size of every time step is enough little, the expression $k_0(p_j T + q_j)$, $j = 1, 2, \ldots, m$ in every element can be considered as $k_0(pT + q)$ in every time step, where p is

constant and q is constant too. The above treatment will be adopted in the following calculation of element variation.

For inner element, according to the control equation of temperature field accompanied by reaction heat, the equation for element variation calculation can be obtained

$$\frac{\partial J^e}{\partial T_l} = \int\int_e \left[k\left(\frac{\partial W_l}{\partial x}\frac{\partial T}{\partial x} + \frac{\partial W_l}{\partial y}\frac{\partial T}{\partial y} \right) - \frac{\rho L k_0}{c_{\text{sivi},0}}(pT+q)c_{\text{sivi}}W_l + \rho c W_l \frac{\partial T}{\partial t} \right] \mathrm{d}x\,\mathrm{d}y \quad (l=i,j,m) \tag{10}$$

According to the definitions of weighting function and shape function, the following formula can be obtained

$$W_l = \frac{\partial T}{\partial T_l} = N_l = \frac{1}{2\Delta}(a_l + b_l x + c_l y) \quad (l=i,j,m) \tag{11}$$

Therefore, $\partial W_l/\partial x$, $\partial W_l/\partial y$ can be calculated based on Eqs. (7)–(9). $\partial T/\partial x$, $\partial T/\partial y$, $\partial T/\partial t$ can be calculated based on Eq. (6).

After a series of equation derivation and area coordinate transformation, the variation equation of inner element can be obtained and expressed in matrix form

$$\left\{\frac{\partial J}{\partial T_l}\right\}^e = [K]^e\{T_l\}^e + [N]^e\left\{\frac{\partial T_l}{\partial t}\right\}^e - \{P_l\}^e \quad (l=i,j,m) \tag{12}$$

where $[K]^e$ and $[N]^e$ are symmetrical and positive definite matrix, $\{P_I\}^e$ is column vector determined by reaction heat.

For outer element, according to the control equation of temperature field accompanied by reaction heat and the thermal boundary condition, the equation for element variation calculation can be obtained

$$\frac{\partial J^e}{\partial T_l} = \int\int_e \left[k\left(\frac{\partial W_l}{\partial x}\frac{\partial T}{\partial x} + \frac{\partial W_l}{\partial y}\frac{\partial T}{\partial y} \right) - \frac{\rho L k_0}{c_{\text{sivi},0}}(pT+q)c_{\text{sivi}}W_l + \rho c W_l \frac{\partial T}{\partial t} \right] \mathrm{d}x\,\mathrm{d}y - \int_{jm} k W_l \frac{\partial T}{\partial n}\mathrm{d}s \quad (l=i,j,m) \tag{13}$$

In contrast to the variation Eq. (10) of inner element, there is a line integral in the variation Eq. (13) of outer element.

According to the research on the thermal boundary condition in the former article, based on the definitions of weighting function and interpolating function of temperature and shape function, the line integral can be calculated. Therefore, the variation equation of outer element, with the third kind of thermal boundary condition or with the fourth kind of thermal boundary condition, can be obtained. The form is similar with Eq. (12). But the specific arithmetic expression of every element in matrix $[K]^e$ and $[N]^e$ and vector $\{P_l\}^e$ for outer element is different from the corresponding one for inner element.

5. Calculation of collectivity synthesis

It can be seen that the number of algebraic equations is n and every equation is composed of accumulative calculation of all element variation from the following equation of collectivity synthesis

$$\frac{\partial J^D}{\partial T_l} = \sum_{e=1}^{E}\frac{\partial J^e}{\partial T_l} = 0 \quad (l=1,2,\ldots,n) \tag{14}$$

After a series of derivation, the equation of collectivity synthesis for calculating the temperature field accompanied by reaction heat can be obtained

$$[K]\{T\}_t + [N]\left\{\frac{\partial T}{\partial t}\right\}_t = \{P\}_t \tag{15}$$

where the subscript t denotes that all the column vectors fetch their values at the same time t.

The time domain is divided by backward difference method, thereby the arithmetic expression for calculating the column vector $\{\partial T/\partial t\}_t$ can be obtained

$$\left\{\frac{\partial T}{\partial t}\right\}_t = \frac{1}{\Delta t}(\{T\}_t - \{T\}_{t-\Delta t}) + \mathrm{O}(\Delta t) \tag{16}$$

The truncation error $\mathrm{O}(\Delta t)$ is ignored, and Eq. (16) is fit into Eq. (15), the equation of collectivity synthesis for calculating temperature field can be obtained, as shown below

$$\left([K] + \frac{[N]}{\Delta t}\right)\{T\}_t = \{P\}_t + \frac{[N]}{\Delta t}\{T\}_{t-\Delta t} \tag{17}$$

where $[K]$, $[N]$, $\{P\}_t$ and $\{T\}_{t-\Delta t}$ are known. Therefore, the temperature field $\{T\}_t$ at the time t can be solved by matrix operation method.

6. Procedures of numerical simulation

The whole finite element simulation includes two kinds of iterative computation. One is that the temperature fields of silicone rubber and LOM prototype are respectively iterated, the other is that the thermal coupling calculation of silicone rubber and LOM prototype is iterated. The implementation procedures are listed below:

1. The temperature field of silicone rubber is computed by alternative manner. First, the uniform temperature fields of silicone rubber and LOM prototype are initialized as $T_{\text{SR0}}$and T_{LOM0} (the initialization is needed only in the first time step). Second, the heat-flow density on the boundary between silicone rubber and LOM prototype is calculated based on the equation

$$q_2 = h_c(T - T_{\text{LOM}})|_\Gamma \tag{18}$$

Third, the temperature field of silicone rubber is computed by finite element method, then the judgement on permissibility of relative differences of all nodal temperatures in fore-and-after computation is formed. If the relative differences are not within the tolerance range, the iterative computation is to be done again. Fourth, according to Eq. (18), the heat-flow density on the boundary is calculated again, and according to the principle of heat flow continuity, its negative value is taken as the thermal boundary condition of LOM prototype.

2. The analogous method is adopted, the temperature field of LOM prototype is computed by alternative manner. After the convergence solution is got, according to Eq. (18), the heat-flow density on the boundary is calculated again, and it is taken as the thermal boundary condition of silicone rubber.
3. The above procedures are repeated until the convergence solution of the thermal coupling calculation of silicone rubber and LOM prototype is achieved. Here, the so-called convergence should be judged by the criterion: on the boundary between silicone rubber and LOM prototype, the relative nodal temperatures and heat-flow densities should be respectively equal (within a certain tolerance range).
4. Incremental theory is adopted, then the increment of the vulcanization ratio of the reactant is calculated in current time step.
5. The fulldose of the vulcanization ratio f_V on every node from the beginning to the current time step is calculated, which is compared with the value $f_{V,c}$ (the fulldose of the vulcanization ratio corresponding to gel point). If $f_V < f_{V,c}$ on a certain node, the numerical computation expressions of the crosslinking structure parameters before gel point are adopted to calculate molecular weight of sol and crosslinking degree of sol, the sol fraction is regarded as one, the crosslinking degree of gel and gel fraction are regarded as zero. If $f_V \geq f_{V,c}$ on a certain node, the numerical computation expressions of the crosslinking structure parameters after gel point are adopted to calculate the crosslinking structure parameters.
6. The minimum value of the fulldoses of the vulcanization ratio $f_{V,min}$ on all nodes from the beginning to the current time step is calculated, which is compared with the ideal value $f_{V,i}$ (the fulldose of the vulcanization ratio corresponding to optimum vulcanization effect). If $f_{V,min} < f_{V,i}$ the program will return to procedure (1) to perform the finite element simulation in the next time step. If $f_{V,min} \geq f_{V,i}$ the program will transfer into the post-processing part to calculate the mechanical properties.

According to the above simulation theory and procedures, the computer-aided engineering software, named MSRVM 4.1, has been designed.

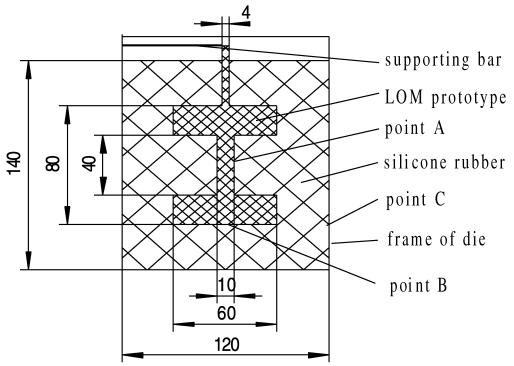

Fig. 3. Sketch of hot vulcanizing (unit: mm).

7. Example and verification

7.1. Example of engineering application

According to the requirements of a certain service contract, the geometric model of a certain artwork is designed with software UGII, then paper is used as moulding material, the LOM prototype of the artwork is manufactured with rapid prototyping equipment HRP-III. At the same time, as shown in Fig. 3, the numerical simulation of the vulcanization process is performed with software MSRVM 4.1. The curves of temperature versus time and vinyl concentration versus time and vulcanization ratio versus time and sol fraction versus time and crosslinking degree versus time of three representative points are shown in Figs. 4–8.

It can be seen from Figs. 4–8 that the temperature and vulcanization ratio and crosslinking degree increase with the time increase, and that the vinyl concentration and sol fraction decrease with the time increase.

The temperature and vulcanization ratio and crosslinking degree of point C are largest, the vinyl concentration and sol fraction of point C are smallest among the three points at the same time. The characteristics of point A are contrary to point C.

7.2. Hardness test and discussion

According to the structure and shape and dimension as

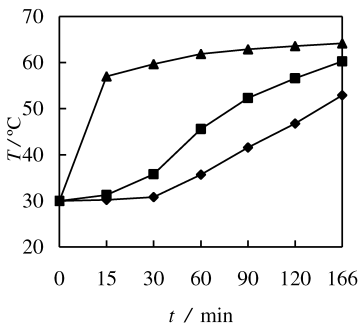

Fig. 4. Curves of temperature versus time (–◆– represents point A, –■– represents point B, –▲– represents point C).

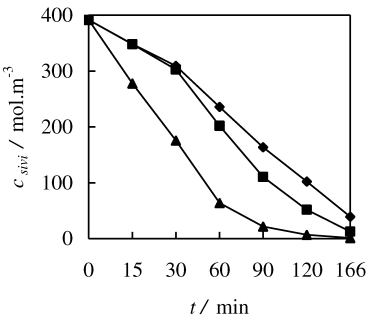

Fig. 5. Curves of vinyl concentration versus time (–◆– represents point A, –■– represents point B, –▲– represents point C).

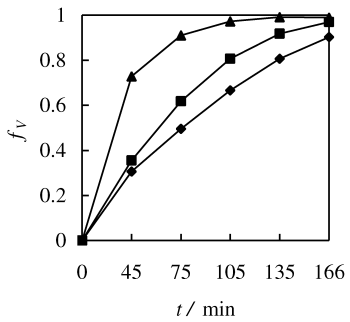

Fig. 6. Curves of vulcanization ratio versus time (–◆– represents point A, –■– represents point B, –▲– represents point C).

shown in Fig. 3, the above-mentioned silicone rubber material is used as mould material, the temperature of electric oven is set for 65 °C, five kinds of silicone rubber moulds have been manufactured, respectively, corresponding to five kinds of vulcanization time 75, 105, 135, 165, and 180 min. Then the hardness H_A of the above-mentioned points is measured immediately. The results are shown in Fig. 9.

It can be seen from Fig. 9 that the hardness of point C is constant since 75 min, the hardness of point B and point A increases gradually. The hardness of point B becomes biggest at about 135 min, The hardness of point A becomes biggest at about 165 min, which is basically coincident with the numerical simulation results as shown in Figs. 6 and 8.

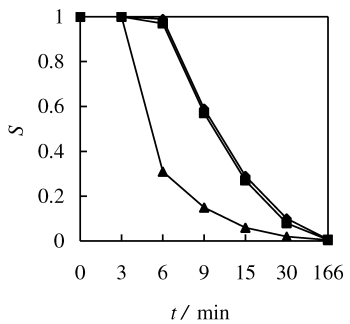

Fig. 7. Curves of sol fraction versus time (–◆– represents point A, –■– represents point B, –▲– represents point C).

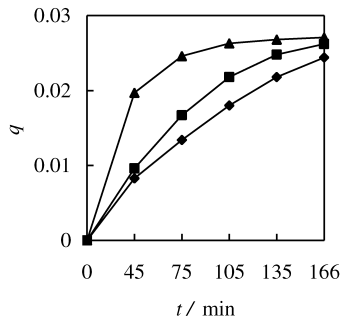

Fig. 8. Curves of crosslinking degree versus time (–◆– represents point A, –■– represents point B, –▲– represents point C).

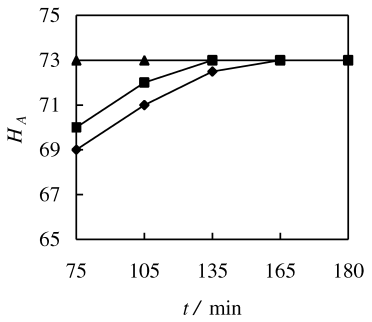

Fig. 9. Experimental curves of hardness versus time.

7.3. Analytical test and discussion

The sol fraction of point C is measured based on gravimetric method. The experimental results are shown as broad-brush curve in Fig. 10. For the convenience of comparison, the theoretical curve of point C in Fig. 7 is redrawn as slimline in Fig. 10.

It can be seen from Fig. 10 that the difference between experimental curve and theoretical curve is little in the forepart of the vulcanization course, but the difference increases with the time increase.

For the phenomenon, the explanation is shown below.

In the forepart of the vulcanization course, the viscosity of the reactant is low, the activity space of polysiloxane molecule is so large that vinyl can freely react chemically with crosslinking agent. Therefore, the chemical reaction is

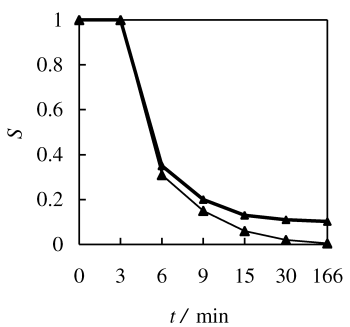

Fig. 10. Experimental curve and theoretical curve.

controlled by kinetics. During the period, the pure kinetic model in the numerical simulation theory can accurately describe the actual vulcanization so that the difference between the experimental data and the calculated data is little.

With the time increase, the viscosity of the reactant increases, and the diffuse motion of the macromolecule and catalyzer progressively influences the reaction rate. The chemical reaction is controlled by reaction mechanism and diffusion mechanism [10–12]. During the period, the pure kinetic model in the numerical simulation theory can only approximately describe the actual vulcanization. Therefore, the experimental data of the sol fraction are bigger than the calculated data, and the difference between them increases with the time increase.

8. Conclusions

1. The numerical simulation theory on silicone rubber vulcanizing is constructed by finite element method.
2. The procedures of the finite element simulation are described in detail, consequently the computer-aided engineering software of the vulcanization process is designed.
3. The rationality of the simulation theory is verified by hardness test and analytical test.

References

[1] Pham DT, Gault RS. Int J Mach Tools Manuf 1998;38:1257.
[2] Yan X, Gu P. Int J Comput Aided Des 1996;28(4):307.
[3] Jia Y, Sun S, Zhao G. Spec Purpose Rubber Prod 2002;23(2):43.
[4] Jia Y, Xue S, Sun S. J Shandong Univ (Engng Sci) 2002;32(2):131.
[5] Chua C, Leong K. Rapid prototyping: principles and applications in manufacturing. New York: Wiley; 1998.
[6] Dickens P. Int J Engng Manuf 1995;209(B):271.
[7] Kong X. Application of finite element method in heat transfer doctrine. Beijing: Science Press; 1998.
[8] Ozisik M. Heat conduction. New York: Wiley; 1980.
[9] Hsiao J. Numer Heat Transfer 1985;8:653.
[10] Lu H, He T, Zhou J. Polym Mater Sci Engng 2001;17(3):98.
[11] Joshi S, Lam Y. Chem Phys Lett 2000;328(4–6):420.
[12] Tobita H, Hamielec A. Polymer reaction engineering. Berlin: Springer; 1989.